Modified Finite Volume Time Domain Method for Efficient Prediction of Radar Cross Section at High Frequencies

Avijit Chatterjee · Rho-Shin Myong

Abstract

The finite volume time domain(FVTD) technique faces serious limitations in simulating electromagnetic scattering at high frequencies due to requirements related to discretization. A modified FVTD method is proposed for electrically large, perfectly conducting scatterers by partially incorporating a time-domain physical optics(PO) approximation for the surface current. Dominant specular returns in the modified FVTD method are modeled using a PO approximation of the surface current allowing for a much coarser discretization at high electrical sizes compared to the original FVTD scheme. This coarse discretization can be based on the minimum surface resolution required for a satisfactory numerical evaluation of the PO integral for the scattered far-field. Non-uniform discretization and spatial accuracy can also be used in the context of the modified FVTD method. The modified FVTD method is aimed at simulating electromagnetic scattering from geometries containing long smooth illuminated sections with respect to the incident wave. The computational efficiency of the modified FVTD method for higher electrical sizes are shown by solving two-dimensional test cases involving electromagnetic scattering from a circular cylinder and a symmetric airfoil.

Key words : Computational Electromagnetics(CEM), Finite Volume Time Domain(FVTD), Hybrid Method, Physical Optics(PO), Radar Cross Section(RCS), Aerospace Configuration.

I. Introduction

The finite volume time domain(FVTD) method, which can be considered a subset of the finite element time domain(FETD) method[1], for solving Maxwell's equations in the time-domain was originally proposed by Shankar[2],[3]. Characteristic based numerical techniques are usually used in the FVTD framework to solve the time-domain Maxwell's equations posed as a set of hyperbolic conservation laws written in a total field form. The time-dependent Euler equations of gas dynamics are normally solved using a similar approach, and this similarity accounts for some of the popularity of the FVTD technique for aerospace applications where this method is increasingly being applied to solve for electromagnetic scattering from aerospace configurations. Higher-order numerical techniques originally developed for the numerical solution of the time-dependent Euler equations can be adapted for use in computational electromagnetics in the FVTD framework[4]. The FVTD technique also has inherent advantages when dealing with complex geometries, broad-band signals and diverse material properties making it an attractive option for the numerical simulation of electromagnetic scattering from complex configurations with varying material properties. But despite these advantages, the FVTD technique is far from being used for routine estimation of radar cross section(RCS) of an aerospace configuration, especially in a design cycle environment. The major limitation of the FVTD technique is the requirement of large computational time at higher frequencies, limiting its application for RCS prediction of realistic geometries at frequency bands relevant for aerospace applications.

Hybrid methods which combine the advantages of two different numerical techniques for a single application are increasingly being used in computational electromagnetics. Hybrid methods have been proposed based on the combination of rigorous techniques like method of moments(MOM) and finite difference time domain(FDTD) with ray or current based high-frequency asymptotic methods for increased computational efficiency when solving for electrically large scatterers[5]~[8]. The advantage of the FDTD technique in dealing with material properties has seen it being hybridized with the more computationally efficient MOM technique[9] while the ability of the FVTD scheme in dealing with complex geometries has led to hybrid FDTD-FVTD formulations [10].

In the present work, a higher-order FVTD method is modified for the numerical simulation of electromagnetic scattering from electrically large, perfectly conducting scatterers. The proposed modification leads to a current-

Manuscript received June 26, 2008 ; revised August 20, 2008. (ID No. 20080626-025J)

Research Center for Aircraft Parts Technology and School of Mechanical and Aerospace Engineering, Gyeongsang National University, Gyeongnam, Korea.

based hybrid technique in the time-domain combining the higher-order FVTD scheme with the high-frequency asymptotic physical optics(PO) method. This modification seeks to improve the computational efficiency of the original FVTD method when dealing with electromagnetic scattering at high frequencies by using the PO approximation of the surface current on smooth illuminated parts of the scatterer. In the modified FVTD method, equivalent surface currents on a perfectly conducting scatterer are evaluated partly based on a regular higher-order FVTD calculation, a PO approximation, and a combined FVTD-PO estimation. The modified FVTD method uses the above mentioned formulations for evaluating surface currents on different parts of the same scatterer, unlike previous attempts at combining the FDTD and PO in the time domain where the existence of multiple scatterers of different electrical sizes are assumed and treated appropriately by either the FDTD or the PO method[7],[8]. The modified FVTD method is aimed at perfectly conducting scatterers with back-scattered field patterns dominated by specular reflection from electrically large smooth regions. Such geometries in the form of drop tanks, missiles, nose radomes are frequently encountered in aerospace applications. Hybrid MOM-PO techniques in the frequency domain have also been previously proposed to deal with geometries like the nose radome at high frequencies where apart from the nose tip the surface geometry can be considered to be locally planar[6]. In the modified FVTD method, the dominant back-scatter pattern consisting of specular reflections from electrically large smooth sections of the scatterer are modeled mainly using a PO approximation for the surface current. The PO approximation usually requires an overall resolution of 2~4 points-per-wavelength(PPW) on the scatterer surface with requirements lower for near-specular regions[11], as for the PO approximation in the present context. These restrictions result from requirements of a satisfactory numerical evaluation of the PO integral[11] to obtain the scattered far-field from PO approximated surface currents. In contrast, the volume based FDTD and FVTD methods usually require a resolution of 15~20 PPW mainly due to problems of numerical dispersion [12], and can be prohibitive for high-frequency applications. The much coarser discretization on the surface of the scatterer usually required by the PO approximation compared to volume based FVTD/FDTD techniques is exploited in two different ways in the present modified FVTD method for high-frequency computations. Since the dominant specular returns for the modified FVTD method are modeled based on a PO approximation, FVTD computations in the modified method can be done on a much coarser volume discretization essentially dictated by the surface resolution of 2~4 PPW for the PO approximation. Alternatively, a non-uniform mesh can be employed for the modified FVTD method with a coarse resolution of 2~4 PPW used in parts of the computational domain containing surfaces modeled using a PO approximation and finer discretization elsewhere. Both these approaches are explored in the modified FVTD method leading to substantially reduced computational effort as compared to the original FVTD scheme for scatterers with electrically large smooth regions. This coarse discretization utilized in the modified FVTD method based on the PO resolution of 2~4 PPW can also be considered the minimum discretization required by a FVTD scheme to satisfactorily predict the scattered far- field in the absence of discretization errors.

In the modified FVTD method, uniform higher-order spatial accuracy is not employed, and higher-order accuracy is limited to parts of the computational domain involving a FVTD or FVTD-PO approximation of the surface current with a first-order spatial accuracy used elsewhere. The modified FVTD technique in the present work uses an essentially non-oscillatory(ENO)[13],[14] based spatial discretization with which arbitrary higher order accuracy can be achieved. Results are presented for two-dimensional cylinder and airfoil subjected to incident harmonic, transverse electric(TE) and transverse magnetic(TM) illumination at high electrical sizes. The smooth geometry of the circular cylinder is used mainly to show the efficacy of the modified FVTD technique in predicting the RCS on a much coarser discretization compared to the original higher-order FVTD scheme. It is well known that the PO method for modeling scattering from a conducting body leads to erroneous contributions due to discontinuity in the surface current at the shadow boundary[15], the failure of the basic PO method to deal with edge discontinuities in the surface geometry is also well documented in literature[16]. The case of a NACA 0012 airfoil illuminated from the trailing edge is presented as an example of the modified FVTD method, which partly includes a PO approximation for the surface current, being able to correctly predict electromagnetic scattering in the presence of a geometric discontinuity where the basic PO method fails.

Ⅱ. Numerical Schemes

2-1 Governing Equations

The three-dimensional Maxwell's curl equations, in the differential form in free space, can be expressed as

$$\frac{\partial B}{\partial t} = -\nabla \times E \tag{1}$$

$$\frac{\partial D}{\partial t} = \nabla \times H - J_i \tag{2}$$

where $\boldsymbol{B}$ is the magnetic induction, $\boldsymbol{E}$ the electric field vector, $\boldsymbol{D}$ the electric field displacement, and $\boldsymbol{H}$ the magnetic field vector. $\boldsymbol{J_i}$ is the impressed current density vector, $\boldsymbol{D}=\varepsilon \boldsymbol{E}$, $\boldsymbol{B}=\mu \boldsymbol{H}$ with ε and μ respectively the permittivity and permeability in free space. The Maxwell's equations can be recasted in a conservative total field form as[1]~[4]

$$u_t + f u_x + g u_y + h u_z = s \tag{3}$$

where subscripts indicate partial derivatives with respect to time t and space (x, y, z) and

$$u=\begin{pmatrix} B_x \\ B_y \\ B_z \\ D_x \\ D_y \\ D_z \end{pmatrix} \quad f=\begin{pmatrix} 0 \\ -D_z/\varepsilon' \\ D_y/\varepsilon' \\ 0 \\ B_z/\mu' \\ -B_y/\mu' \end{pmatrix} \quad g=\begin{pmatrix} D_z/\varepsilon' \\ 0 \\ -D_x/\varepsilon' \\ -B_z/\mu' \\ 0 \\ B_x/\mu' \end{pmatrix}$$

$$h=\begin{pmatrix} -D_y/\varepsilon' \\ D_x/\varepsilon' \\ 0 \\ B_y/\mu' \\ -B_x/\mu' \\ 0 \end{pmatrix} \quad s=\begin{pmatrix} 0 \\ 0 \\ 0 \\ -J_{ix} \\ -J_{iy} \\ -J_{iz} \end{pmatrix} \tag{4}$$

Subscripts x, y, z in the above vectors denote components in the respective Cartesian coordinate directions. In two dimensions, Maxwell's equations can be split into two sets of systems[17]. These are the equations for TM and TE waves. The two-dimensional conservative form is written as

$$u_t + f_x + g_y = s \tag{5}$$

The vectors in equation (5) for the TM waves are

$$u=\begin{pmatrix} B_x \\ B_y \\ D_z \end{pmatrix} \quad f=\begin{pmatrix} 0 \\ -D_z/\varepsilon \\ -B_y/\mu \end{pmatrix} \quad g=\begin{pmatrix} D_z/\varepsilon \\ 0 \\ B_x/\mu \end{pmatrix}$$

$$s=\begin{pmatrix} 0 \\ 0 \\ -J_z \end{pmatrix} \tag{6}$$

while that for the TE waves are

$$u=\begin{pmatrix} B_z \\ D_x \\ D_y \end{pmatrix} \quad f=\begin{pmatrix} D_y/\varepsilon \\ 0 \\ B_z/\mu \end{pmatrix} \quad g=\begin{pmatrix} -D_x/\varepsilon \\ -B_z/\mu \\ 0 \end{pmatrix}$$

$$s=\begin{pmatrix} 0 \\ -J_x \\ -J_z \end{pmatrix} \tag{7}$$

2-2 Finite Volume Time Domain Technique

The FVTD technique usually solves the integral form of the conservative Maxwell's equations in a scattered field formulation with the incident field assumed to be a solution of the Maxwell's equations in free space. Integrating the differential form of the conservation law [18] represented by equation (3), in the absence of a source term over an arbitrary control volume Ω,

$$\frac{\partial \int_\Omega u^s dV}{\partial t} + \int_\Omega \nabla \cdot (F(u^s)) dV = 0. \tag{8}$$

Here $\boldsymbol{F}$ is the flux vector with components f, g, h respectively in the Cartesian x, y, z directions. Applying the divergence theorem, the integral form of the conservation law is obtained as

$$\frac{\partial \int_\Omega u^s dV}{\partial t} + \oint_S F(u^s) \cdot \hat{n} dS = 0 \tag{9}$$

and used to formulate the problem in the FVTD framework. $\boldsymbol{F}$ is the flux vector, $\hat{n}$ the outward unit normal vector, superscript 's' indicates scattered field variables. For three-dimensional problems, the domain can be discretized into hexahedral cells and the integral form applied to each cell. The corresponding discretization for 2D problems consists of quadrilateral cells. The discretized form for the k-th cell in the cell-centered formulation in three-dimensions is

$$\Omega_k \frac{d\overline{u_k}^s}{dt} + \sum_{j=1}^{6} [(F(u^s) \cdot \hat{n}S)_j]_k = 0 \tag{10}$$

where $\overline{u_k}^s$ indicates the volume average of u_s over cell k and $[(F(u^s) \cdot \hat{n}S)_j]_k$ the average flux through face j of cell k. The equivalent two-dimensional form solved for in the present work is

$$A_k \frac{d\overline{u_k}^s}{dt} + \sum_{j=1}^{4} [(F(u^s) \cdot \hat{n}S)_j]_k = 0 \tag{11}$$

Equations (10) and (11) represent generic systems of hyperbolic conservation laws discretized in a finite volume framework and can be solved using a variety of numerical schemes. Numerical schemes usually used to solve hyperbolic conservation laws either have the space and time discretization coupled as in the Lax-Wendroff class of schemes or have them treated separately in a method of lines approach. The spatial discretization followed by a numerical technique is reflected in the representation of the numerical flux function $(F(u^s) \cdot \hat{n})_{num}$ which approximates $F(u^s) \cdot \hat{n}$ in equations (10) and (11). Numerical schemes in the method of lines approach can also differ in the time-integration procedure followed to advance the above equations in time.

In the present work, the two dimensional Maxwell's equations represented by its discretized form in equation (11), are solved in the FVTD framework using a higher

order ENO[13],[14] scheme for spatial discretization along with a second order Runge-Kutta time integration. Higher order accuracy in evaluating the numerical flux function in equation (11) is achieved through an ENO reconstruction, more information regarding the ENO scheme and its adaptation to the FVTD framework can be found in Ref. [19]. For perfect electric conductors solved for in the present work, the total tangential electric field $\hat{n} \times E = 0$ on the conducting surface. Standard characteristic boundary conditions can be implemented at the outer boundary with the scattered field variables being taken as zero in the far field.

2-3 Modified FVTD Method

Based on the equivalence principle, the surface current density vector on the scatterer surface in the time domain is defined as

$$J_{sur}(r, t) = \hat{n} \times H(r, t) \tag{12}$$

This can be decomposed into contributions from the scattered (s) and incident (i) fields and written as

$$J_{sur}(r, t) = J^{i}_{sur}(r, t) + J^{s}_{sur}(r, t) \tag{13}$$

where

$$J^{i}_{sur}(r, t) = \hat{n} \times H^{i}(r, t) \tag{14}$$

and

$$J^{s}_{sur}(r, t) = \hat{n} \times H^{s}(r, t) \tag{15}$$

In the modified FVTD method, the surface of the scatterer is divided into FVTD, PO and "transition" regions based on the evaluation of the surface current. The surface current density in the FVTD region is defined as

$$J^{FVTD}_{sur}(r, t) = J^{i}_{sur}(r, t) + J^{s'}_{sur}(r, t) \tag{16}$$

where (s') indicates the scattered field computed using a higher order FVTD technique. Replacing the scattered field in equation (13) by the local incident field leads to the PO current

$$J^{PO}_{sur}(r, t) = J^{i}_{sur}(r, t) + J^{i}_{sur}(r, t) \tag{17}$$

defined on PO regions. The PO current is commonly used to approximate the surface current density on lit smooth regions of a electrically large, perfectly conducting scatterer in the PO method. The scattered field in equation (13) is replaced by a linear combination of the local incident field and the FVTD computed scattered field to yield the current in the transition region

$$J^{trans}_{sur}(r, t) = J^{i}_{sur}(r, t) + \zeta J^{i}_{sur}(r, t) + (1 - \zeta) J^{s'}_{sur}(r, t) \tag{18}$$

with $\zeta = [0, 1]$. This of course assumes $J^{trans}_{sur}(r(\zeta = 0), t) = J^{FVTD}_{sur}(r, t)$ and $J^{trans}_{sur}(r(\zeta = 1), t) = J^{PO}_{sur}(r, t)$. For the modified FVTD method, the surface current density on long smooth lit regions of the scatterer is defined using the PO approximation J^{PO}_{sur} while that in the shadow regions and in areas containing edge discontinuities it is taken as the FVTD computed current J^{FVTD}_{sur}. J^{trans}_{sur} is used to define the surface current density in the transition region connecting the FVTD and PO currents. The surface current density vectors defined above are calculated in the time domain and the complex current in the frequency domain for the complete scatterer surface computed from the time history using a Fourier transform. Predicting the RCS requires the scattered field intensity at infinity which is obtained from the complex currents calculated on the surface of the scatterer through a near-to-far field transformation (the Stratton-Chu integral)[17],[20],[21]. When equivalent surface currents in the frequency domain are based purely on a PO approximation, the radiation integrals in the near-to-far field transformation are also referred to as the PO integral[11].

In the present modified method, FVTD computations are required for the entire computational domain in order to define surface currents J^{FVTD}_{sur} and J^{trans}_{sur} on only the FVTD and transition regions of the scatterer surface. But the FVTD analysis can be performed on a relatively coarse discretization since the dominant specular returns of electrically large smooth parts of scatterers, amenable to the present method, are modeled using the PO approximation for the surface current. The volume discretization used for the FVTD analysis in the present method is based on a resolution of 2~4 PPW usually required on the scatterer surface for numerical evaluation of the PO integral[11]. This is in sharp contrast to the average resolution of 15~20 PPW, required by FVTD and FDTD schemes due to problems related to numerical dispersion, and can lead to a substantially reduced computational effort at higher frequencies. Even without an uniformly coarse discretization for the FVTD analysis, savings in computational time in the present method can still be obtained by restricting finer discretization for the FVTD analysis to only parts of the computational domain containing surfaces with currents defined by J^{FVTD}_{sur} or J^{trans}_{sur}, as is shown subsequently. In the present method, a higher order spatial discretization for the FVTD scheme is not applied uniformly. A third-order spatial accuracy using an ENO[15],[16] reconstruction is used selectively in the computational domain containing parts of the scatterer surface with currents defined as or J^{trans}_{sur}. A first-order upwind scheme is used for the rest

of the domain.

The modified FVTD method can be summarized in the following steps.

1) FVTD computations are carried out on an uniformly coarse mesh or on a non-uniform mesh based on the definition of the surface current. A coarse mesh and first-order spatial accuracy for FVTD computations is always employed in the part of the computational domain containing PO approximation of surface current.

2) Surface current densities are evaluated in the time-domain. J_{sur}^{PO}, J_{sur}^{FVTD} and J_{sur}^{trans} are calculated at appropriate locations on the scatterer surface as described above.

3) The complex surface currents for the entire scatterer surface are obtained using a Fourier transform based on the time history of the above-defined currents.

4) The RCS for the scatterer obtained using a near-to-far-field transformation.

Ⅲ. Numerical Solutions

3-1 Circular Cylinder

The smooth geometry of the circular cylinder is used to demonstrate the efficacy of the modified FVTD method compared to the original FVTD scheme at high electrical sizes. Fig. 1 shows a two-dimensional perfectly conducting cylinder subjected to continuous harmonic incident TE or TM wave. The lit and shadow regions for the cylinder are defined respectively as $[\pi/2, 3\pi/2]$ and $[\pi/2, -\pi/2]$ with $\theta=\pm\pi$ the monostatic point in Fig. 1. For TM illumination, the entire lit surface is considered the PO region with surface current defined as J_{sur}^{po}. The higher-order FVTD computed current J_{sur}^{FVTD} is valid over most of the shadow surface except for the small transition region near the shadow boundary where the surface current is defined as J_{sur}^{trans}. The transition region is typically taken to be few wavelengths long. A third-order ENO based spatial discretization is considered for the computational domain containing the shadow region while a first-order upwind scheme is used elsewhere as shown in Fig. 1 along with the FVTD, PO and transition regions. For TE illumination, an identical strategy is followed except that the transition region is located towards the lit section at the shadow boundary. The transition regions are located differently on the circular cylinder for TM and TE cases due to the much greater loss in accuracy for a FVTD based coarse grid TM solution in the non-specular region as compared to its TE counterpart. Since the transition region for the TM illumination is towards the shadow area, the transition current in equation (18) can also be better approximated as,

$$J_{sur}^{trans}(r,t)=J_{sur}^{i}(r,t)+\zeta J_{sur}^{i}(r_{sb},t)+(1-\zeta)J_{sur}^{s}(r,t) \quad (19)$$

where $r=r_{sb}$ indicates the appropriate shadow boundary.

Computations are initially carried out for the modified FVTD method on an uniformly coarse discretization based on approximately the minimum resolution required on the surface of the scatterer for a satisfactory numerical evaluation of the PO integral. An 'O' type grid is employed in the 2D computational domain with the number of points in the radial direction fixed at 50. The 'O' type grid is a typical boundary fitted mesh used to discretize convex geometries and is shown schematically in Fig. 2. Results are presented for TM and TE illumination for electrical sizes corresponding to $a/\lambda=9.6$ and $a/\lambda=14.4$, where a is the cylinder radius, and λ is the wavelength of the continuous harmonic incident TE or TM wave. The coarse discretization for the modified FVTD method for both electrical sizes is obtained by taking 200 uniformly spaced grid points in the circumferential direction. This implies surface resolutions of respectively 3.1 and 2.2 PPW at a/λ of 9.6 and 14.4, and is approximately the minimum surface resolution requi-

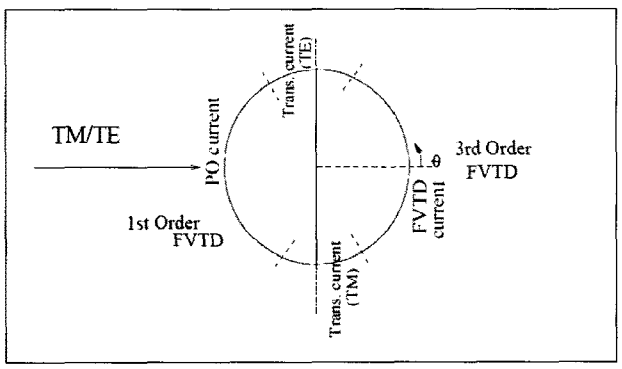

Fig. 1. Scattering from a circular cylinder.

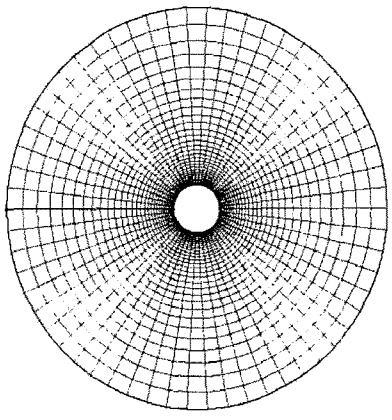

Fig. 2. O-grid circular cylinder, schematic.

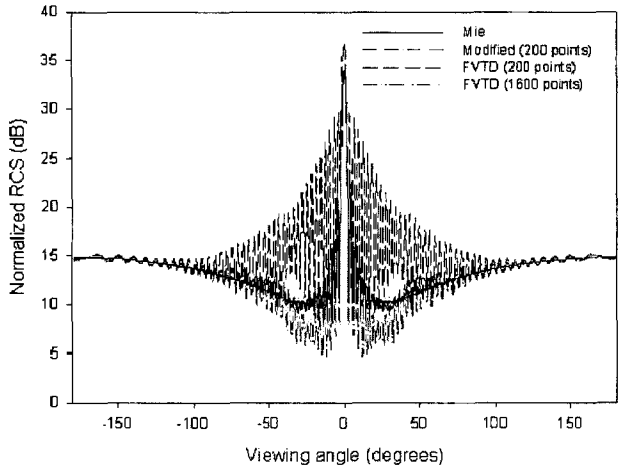

Fig. 3. Bistatic RCS circular cylinder, TM wave $a/\lambda =$ 9.6.

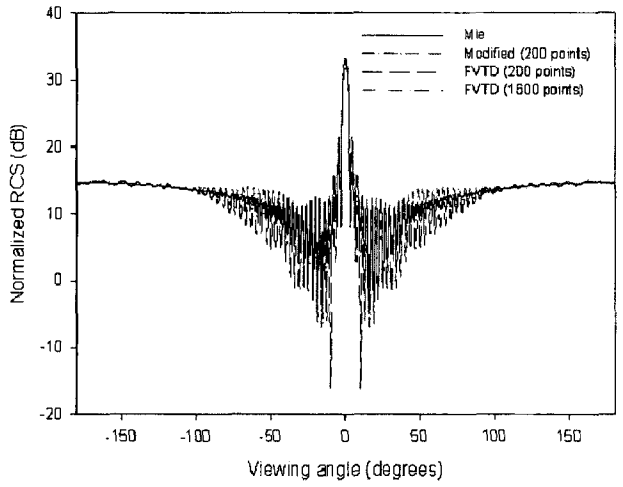

Fig. 4. Bistatic RCS circular cylinder, TE wave $a/\lambda =$ 9.6.

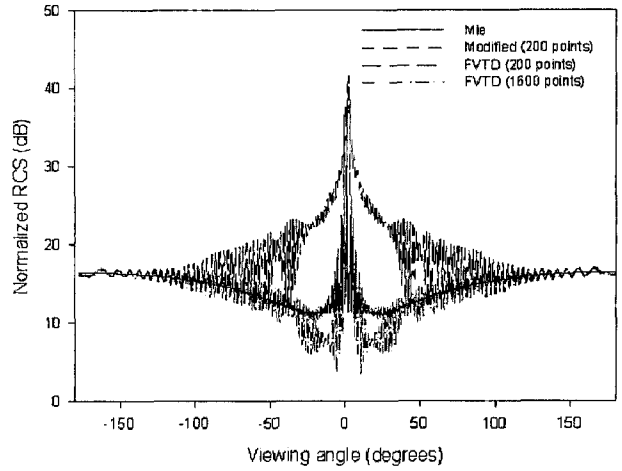

Fig. 5. Bistatic RCS circular cylinder, TM wave $a/\lambda =$ 14.4.

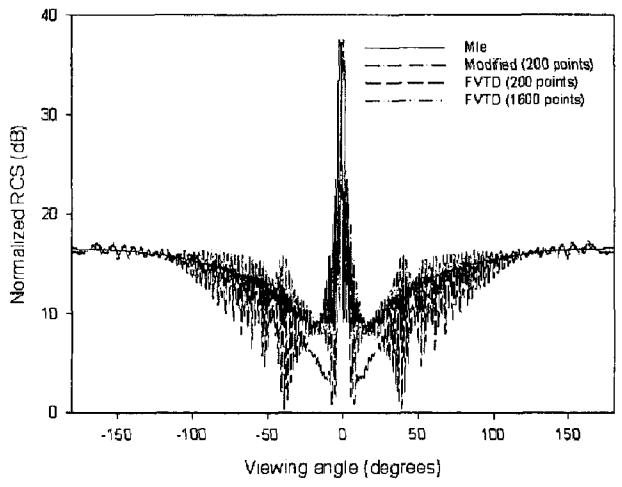

Fig. 6. Bistatic RCS circular cylinder, TE wave $a/\lambda =$ 14.4.

red to numerically evaluate the PO integral.

Figs. 3 and 4 respectively show the bistatic RCS(normalized with respect to the wavelength) for the TM and TE case at a/λ=9.6. Results are compared for a modified FVTD method on a coarse discretization, a third-order ENO based FVTD method also on the coarse discretization, the Mie or exact solution, and a third order FVTD solution obtained on a fine grid with 1,600 points along the circumferential direction. For both TE and TM cases, the solution with a third-order FVTD scheme on the coarse discretization has a significant deviation from the exact solution. There is a considerable improvement in the solution at the same resolution when a modified FVTD method is used with dominant specular returns modeled with a PO approximation of the surface current. Similarly Figs. 5 and 6 respectively compare the bistatic RCS for TM and TE illumination for a/λ=14.4. There is a further deviation of the FVTD solution from the exact solution which again to a very large extent is corrected by using the modified FVTD method.

Results are also presented for the modified FVTD method on a non-uniform mesh with the non-uniform discretization defined on basis of the surface current. Previous results using the modified FVTD method on an uniform coarse mesh shows an overall good comparison with the exact or Mie series results for the bistatic RCS except at locations very far from the specular region. This is a consequence of the coarse FVTD discretization in the shadow region used to model non-specular returns. This error can also be removed by limiting the coarse mesh to the lit section of the scatterer and using a regular fine mesh in the remaining part of the domain. Figs. 7 and 8 show results for a TM and TE illumination at a/λ =14.4.

The previous coarse grid at 2.2 PPW is retained in most of the lit region involving a PO approximation for

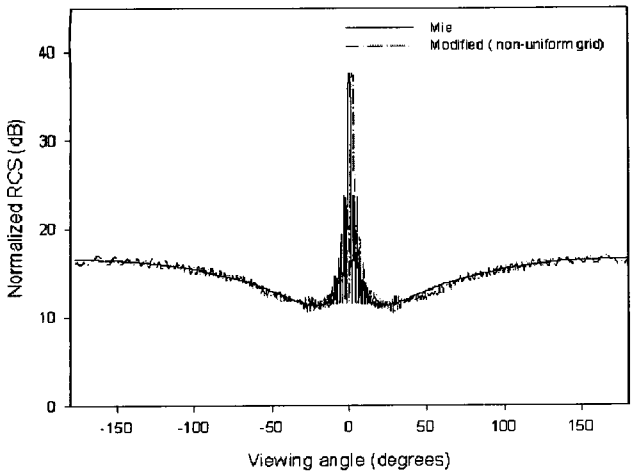

Fig. 7. Bistatic RCS circular cylinder, TM wave $a/\lambda =$ 14.4, non-uniform grid.

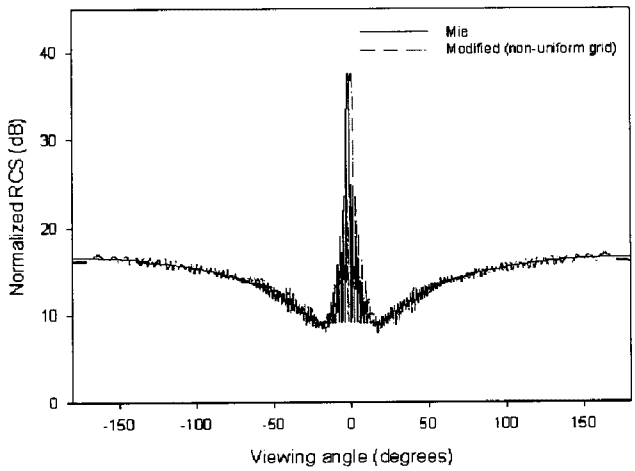

Fig. 8. Bistatic RCS circular cylinder, TE wave $a/\lambda =$ 14.4, non-uniform grid.

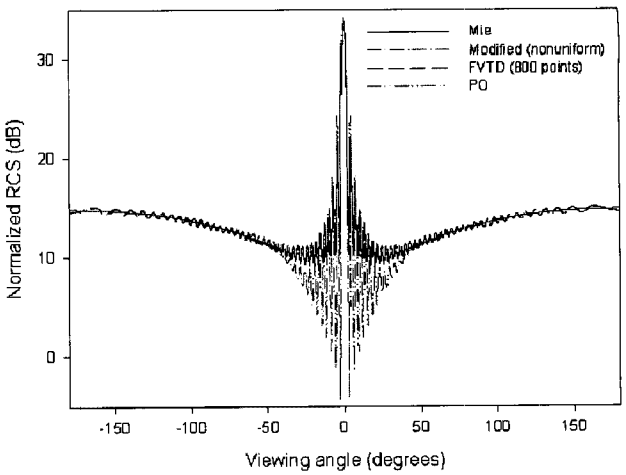

Fig. 9. Bistatic RCS circular cylinder, TM wave $a/\lambda =$ 9.6, non-uniform grid.

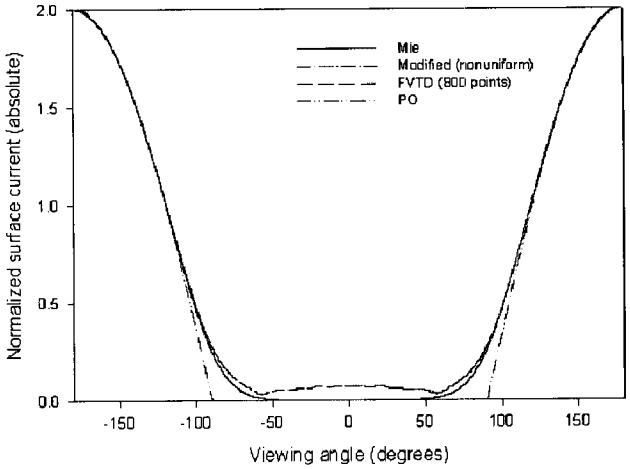

Fig. 10. Distribution of surface current on circular cylinder, TM wave $a/\lambda =9.6$, non-uniform grid.

the surface current. In the shadow region involving a FVTD evaluation of the surface current the previous fine grid is employed. Results are compared for the modified FVTD method on this non-uniform mesh and the Mie series or exact solution and excellent agreement can be seen. Excellent agreement was similarly obtained with Mie series results for $a/\lambda =9.6$ on a non-uniform mesh consisting of coarse mesh with 3.1 PPW on most of the lit region and a fine grid elsewhere as can be seen in Fig. 9 and Fig. 10, which illustrates the distribution of surface current on the cylinder. The modified FVTD method on a non-uniform mesh is computationally more efficient compared to a regular FVTD scheme on an uniform fine grid because of partial use of a coarse mesh and first-order accuracy in the computational domain.

3-2 NACA 0012 Airfoil

The previous example of a circular cylinder was mainly used to illustrate the superior ability of the modified FVTD method in predicting the RCS of electrically large smooth shapes over the original FVTD technique. The modified FVTD method is based on a PO approximation of the surface current on electrically large smooth lit sections of the scatterer.

Electromagnetic scattering from a perfectly conducting NACA 0012 airfoil at high frequencies is used to show the efficacy of the modified FVTD method over the basic PO technique. The airfoil is illuminated from the trailing edge as in Fig. 11. The airfoil geometry shown here is a representation and not drawn to scale. The basic PO technique fails in this case due to the geometric discontinuity at the airfoil trailing edge. In the modified FVTD method, the surface current at and around the trailing edge point is defined as the FVTD current. Transition regions with surface currents defined as in

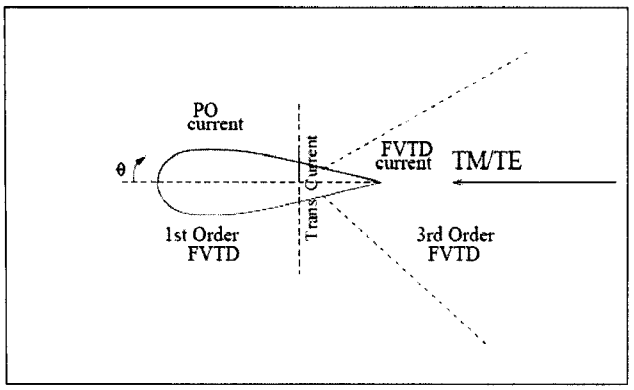

Fig. 11. Scattering from a NACA 0012 airfoil, trailing edge illumination.

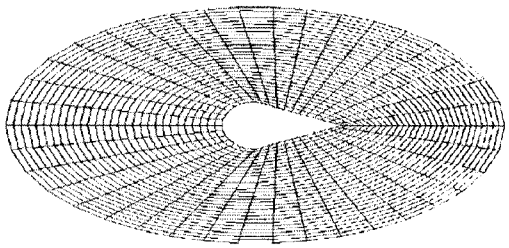

Fig. 12. O-grid airfoil, schematic.

equation (18) connect the FVTD with the PO region defined over the rest of the airfoil, as shown in Fig. 11. It may be noted that the NACA 0012 airfoil has a maximum thickness-to-chord ratio of only 12 % and the leading edge does not cause a regular shadow region to be formed for a trailing edge illumination. Thus, the PO approximation can be considered to be valid at the leading edge under conditions shown in Fig. 11 and as verified in subsequent results.

The NACA 0012 airfoil is again discretized with a body confirming 'O' type mesh and the number of points in the radial direction kept constant at 50. The mesh topology is identical to that used previously for a circular cylinder and shown in Fig. 12. Fig. 13 shows the bistatic RCS for a NACA 0012 airfoil subjected to TM illumination from the trailing edge, $a/\lambda=40$ with a the airfoil chord. The result for the modified FVTD method is shown on a discretization consisting of 400 points around the airfoil (400×50 grid) and compared with a fine grid FVTD solution on a 1,600×50 grid, $\theta=\pm\pi$ indicates the monostatic point. For the modified method, the FVTD region on the airfoil surface ranged from a minimum of 2λ from the trailing edge along the airfoil chord to a maximum of 20λ. Relatively similar results were obtained with the modified FVTD method as this region around the trailing edge was varied. Results are also presented for the NACA 0012 airfoil subject to TE

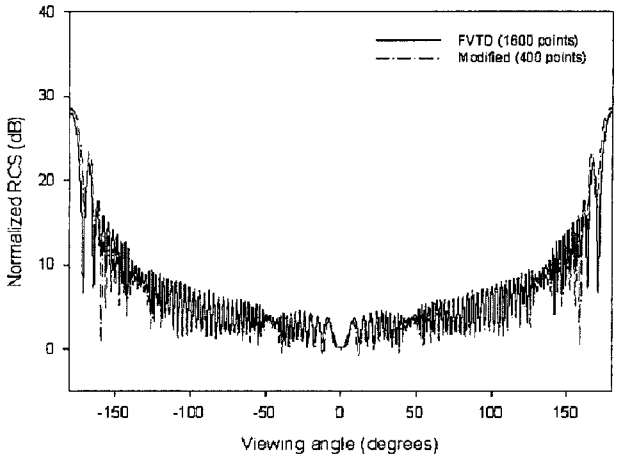

Fig. 13. Bistatic RCS NACA 0012 airfoil, TM wave $a/\lambda=40$.

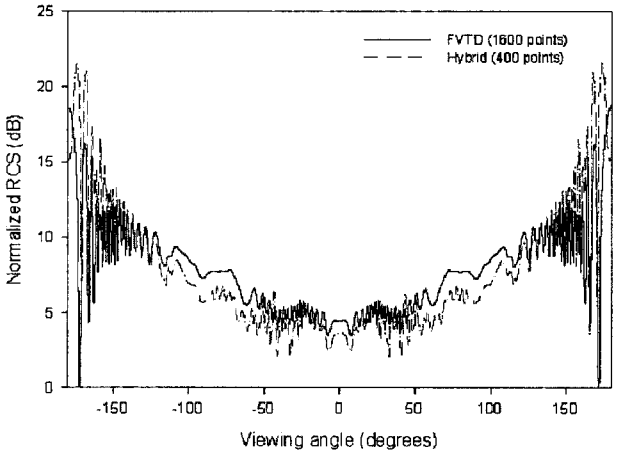

Fig. 14. Bistatic RCS NACA 0012 airfoil, TE wave $a/\lambda=60$.

illumination from the trailing edge for $a/\lambda=60$. Fig. 14 compares the bistatic RCS obtained using the modified FVTD method with a third-order fine grid FVTD solution and again reasonable agreement is obtained.

Ⅳ. Conclusion

The FVTD technique, despite its many advantages, faces serious limitations in simulating electromagnetic scattering at high electrical sizes due to the fine discretization required in terms of points-per-wavelength. A modified FVTD method is proposed based on an asymptotic PO approximation for the surface current on electrically large, smooth, lit parts of a perfectly conducting scatterer. The main emphasis of the present work was on the enhancement of computational efficiency in predicting the radar cross section by developing a hybrid scheme built on merits

of each method(FVTD and PO), rather than on the issue of numerical accuracy. The dominant specular returns at high electrical sizes are modeled using a PO approximation for the surface current allowing a much coarser discretization to be used for the FVTD analysis. The coarser discretization used for FVTD computations in the modified method is dictated by that required for the numerical evaluation of the PO integral for near-specular scattering, and can be close to the maximum Nyquist sampling interval of 2 PPW. This is in contrast to FVTD or FDTD requirements which can be in the range of 15~20 PPW leading to substantial reduction in computational time at higher electrical sizes. A non-uniform mesh, with fine grid restricted to only parts of the computational domain containing FVTD calculated surface currents, can also be employed for the modified FVTD method. The modified FVTD method is aimed at high-frequency electromagnetic scattering from geometries containing long smooth sections where a PO approximation for the surface current can be assumed to be valid.

This work was supported by Korea Research Foundation (KRF-2005-005-J09901) and the Flight Vehicle Research Center (UD070041AD).

References

[1] J. Jin, *The Finite Element Method in Electromagnetics*, John Wiley & Sons, 2002.

[2] V. Shankar, W. F. Hall, and A. H. Mohammadian, "A time-domain differential solver for electromagnetic scattering problems", *Proceedings of the IEEE*, vol. 77, no. 5, pp. 709-721, 1989.

[3] V. Shankar, "A gigaflop performance algorithm for solving Maxwell's equations of electromagnetics", *AIAA*, pp. 91-1578, 1991.

[4] J. S. Shang, "Characteristic-based algorithms for solving the Maxwell equations in the time domain", *IEEE Antennas and Propagation Magazine*, vol. 37, no. 3, pp. 15-25, 1995.

[5] M. Djordjevic, B. M. Notaros, "Higher order hybrid method of moments-physical optics modeling technique for radiation and scattering from large perfectly conducting surfaces", *IEEE Transactions on Antennas and Propagation*, vol. 53, no. 2, pp. 800-813, 2005.

[6] M. A. Abdel Moneum, X. Shen, J. L. Volakis, and O. Graham, "Hybrid PO-MOM analysis of large axisymmetric radomes", *IEEE Transactions on Antennas and Propagation*, vol. 49, no. 12, pp. 1657-1666, 2001.

[7] L. X. Yangi, D. B. Ge, and B. Wei, "FDTD/TDPO hybrid approach for analysis of the EM scattering of combinative objects", *Progress in Electromagnetics Research, PIER 76*, pp. 275-284, 2007.

[8] H. T. Chou, H. T. Hsu, "Hybridization of simulation codes based on numerical high and low frequency techniques for the efficient antenna design in the presence of electrically large and complex structures", *Progress in Electromagnetics Research, PIER 78*, pp. 173-187, 2008.

[9] R. A. Abd-Alhameed, P. S. Excell, and M. A. Mangoud, "A hybrid computational electromagnetics formulation for simulation of antennas coupled to lossy and dielectric volumes", *IEEE Transactions on Antennas and Propagation*, vol. 50, no. 3, pp. 253-269, 2004.

[10] X. Ferrieres, J. P. Parmantier, S. Bertuoul, and A. R. Ruddle, "Application of a hybrid finite difference/ finite volume method to solve an automotive EMC problem", *IEEE Transactions on Electromagnetic Compatibility*, vol. 46, no. 4, pp. 624-634, 2004.

[11] R. J. Burkholder, T. H. Lee, "Adaptive sampling for fast physical optics numerical integration", *IEEE Transactions on Antennas and Propagation*, vol. 53, no. 5, pp. 1843-1845, 2005.

[12] K. S. Yee, J. S. Chen, "The finite-difference time domain(FDTD) anf finite-volume time-domain methods in solving Maxwell''s equations", *IEEE Transactions on Antennas and Propagation*, vol. 45, no. 3, pp. 354-363, 1997.

[13] C. W. Shu, S. Osher, "Efficient implementation of essentially non-oscillatory shock-capturing schemes", *Journal of Computational Physics*, vol. 77, no. 2, pp. 439-471, 1988.

[14] C. W. Shu, S. Osher, "Efficient implementation of essentially non-oscillatory shock-capturing schemes II", *Journal of Computational Physics*, vol. 83, no. 1, pp. 32-78, 1989.

[15] I. J. Gupta, W. D. Burnside, "A physical optics correction for backscattering from curved surfaces", *IEEE Transactions on Antennas and Propagation*, vol. 35, no. 5, pp. 553-561, 1987.

[16] S. W. Lee, "Comparison of uniform asymptotic theory and Ufimtsev's theory of electromagnetic edge diffraction", *IEEE Transactions on Antennas and Propagation*, vol. 25, no. 2, pp. 162-170, 1977.

[17] R. F. Harrington, *Time-Harmonic Electromagnetics Fields*, McGraw Hill, 1961.

[18] R. J. LeVeque, *Numerical Methods for Conservation Laws*, Birkhauser Verlag, 1992.

[19] A. Chatterjee, A. Shrimal, "Essentially nonoscillatory finite volume scheme for electromagnetic sca-

ttering by thin dielectric coatings", *AIAA Journal*, vol. 42, no. 2, pp. 361-365, 2004.
[20] C. A. Balanis, *Advanced Engineering Electro-magnetics*, John Wiley, 1989.
[21] E. F. Knott, J. F. Shaeffer, and M. T. Tuley, *Radar Cross Section*, Artech House, 1993.

Avijit Chatterjee

received the B.Tech. and Ph.D. degrees in the dept. of aeronautical and aerospace engineering from the Indian Institute of Technology, Bombay in 1989 and 1995. He also received a M.S. degree in the dept. of aerospace engineering from the University of Florida in 1990. He worked as a postdoctoral fellow in the faculty of aerospace engineering Technion-Israel Institute of Technology from 1995 to 1997. Currently, he is a full-time research professor at the Research Center for Aircraft Parts Technology in the Gyeongsang National University. His permanent position is an associate professor of the dept. of aerospace engineering at the Indian Institute of Technology, Bombay. His research interests include aerodynamics, computational fluid dynamics and computational electromagnetics and acoustics.

Rho-Shin Myong

received the B.S. and M.S. degrees in the dept. of aeronautical engineering from the Seoul National University in 1987 and 1989, respectively. He received a Ph.D. degree in the dept. of aerospace engineering from the University of Michigan in 1996. Prior to the present position, he worked on the project of a global MHD modeling at the NASA Goddard Space Flight Center from 1997 to 1999 as a NRC research associate. Currently, he is a professor of the school of mechanical and aerospace engineering at the Gyeongsang National University in Jinju. His research interests include modeling and simulation of nonequilibrium fluid flow and heat transfer in space/micro/nano systems, applied aerodynamics and CFD, aircraft survivability and stealth technology.